

Quantum catcher - stopping particles of unknown velocities

S. Schmidt,^{1,*} J. G. Muga,^{2,†} and A. Ruschhaupt^{1,‡}

¹*Institut für Mathematische Physik, TU Braunschweig,
Mendelssohnstrasse 3, 38106 Braunschweig, Germany*

²*Departamento de Química Física, UPV-EHU, Apartado 644, 48080 Bilbao, Spain*

We propose a method to stop particles of unknown velocities by collision with an accelerated wall with trajectory $\sim \sqrt{t}$. We present classical and quantum mechanical descriptions and numerical simulations that show the efficiency of the method.

PACS numbers: 42.50.-p

I. INTRODUCTION

A beam of particles can be slowed down by reflecting them from a potential wall (or “mirror”) moving in the same direction. An early example is the production of an ultracold beam of neutrons colliding with a moving Ni-surface [1]. Moving mirrors for cold atom waves have been also implemented with a time-modulated, blue-detuned evanescent light wave propagating along the surface of a glass prism [2, 3]. More recently, beams of Helium atoms have been slowed down using a Si-crystal on a spinning rotor [4, 7]. Also, Rb atoms have been stopped with a moving magnetic mirror on a conveyor belt [5], which provides a promising mechanism to generate a continuous, intense and slow beam of atoms. There is clearly a great potential for practical applications of such processes and much interest in their fundamental properties and optimization. In most cases the analysis is made with classical trajectories, but quantum motion effects may become important for ultracold atoms, as shown in a recent study on matter-wave/moving-mirror interaction [6]. One more limitation of standard settings so far is that the mirror motion is adapted only to stop a specific initial beam velocity. We may however consider the much more general case in which the initial velocities are broadly distributed, or that they are unknown. Stopping a beam in these conditions is a much more challenging objective, and the central subject of the present paper.

Can we stop a classical particle of unknown velocity with a moving hard wall? The answer is yes and the trajectory of the wall is surprisingly simple, as we shall see in Sect. II. We shall also explore in Sect. III the extent to which the same methodology can be applied in the quantum case, and provide numerical examples.

II. CLASSICAL ENSEMBLE OF NON-INTERACTING PARTICLES

Let us start by assuming a classical point-particle emitted at $x = 0$, $t = 0$, moving with unknown velocity $v \geq 0$ along x . A heavy hard wall (compared to the mass of the particle) moves also with trajectory $x_m(t)$ and initial condition $x_m(0) = 0$. If the particle touches the wall at time t with velocity v_s and the wall is moving with velocity v_m at t , then the final velocity v_f of the particle after the perfect reflection is

$$v_f = -v_s + 2v_m. \quad (1)$$

This can be easily seen in the reference frame in which the mirror is at rest at time t . To fulfill the goal that the particle is at rest in the laboratory frame after the collision, the mirror velocity should be $v_m = v_s/2$ at the time of the collision. Since the trajectory of the particle with velocity $v > 0$ is $x(t) = vt$ and the trajectory of the mirror is $x_m(t)$, the time t_c of the collision is given as a solution of $x_m(t_c) = vt_c$. The condition for stopping the particle is now

$$\frac{dx_m}{dt}(t_c) = \frac{v}{2}.$$

Using $v = x_m(t_c)/t_c$ we get

$$\frac{dx_m}{dt}(t_c) = \frac{x_m(t_c)}{2t_c}.$$

The trajectory for the mirror we are looking for is found as the solution of this ordinary differential equation with the initial condition $x_m(0) = 0$,

$$x_m(t) = \alpha\sqrt{t}, \quad (2)$$

where $\alpha > 0$ is in principle arbitrary, although its value will determine the location and time of the particle-mirror collision, which is quite important in a practical implementation with limited space and time. Such a moving wall will stop particles starting at the origin and moving with positive velocity independent of their initial velocity, see also Fig. 1. Instead of α we will deal with more intuitive parameters: we assume a final time t_f , this may be a maximal time we are ready to consider

*Electronic address: soenke.schmidt@tu-bs.de

†Electronic address: jg.muga@ehu.es

‡Electronic address: a.ruschhaupt@tu-bs.de

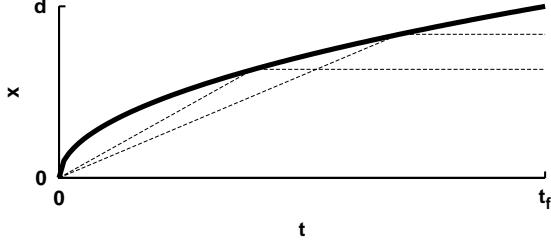


FIG. 1: Scheme of the stopping of classical particles: a hard wall moving with trajectory $x_m(t) = d\sqrt{t/t_f}$ (solid line); examples of two particle trajectories with different initial velocities (dashed lines).

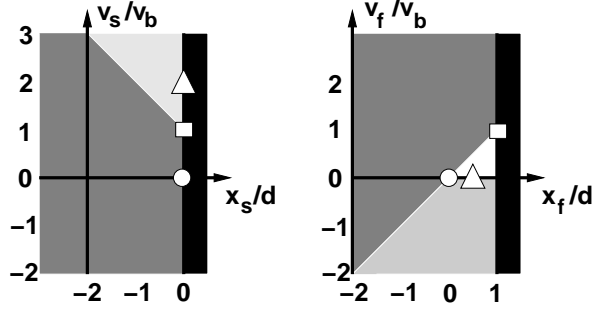


FIG. 2: Scheme of the transformation between initial parameters and final parameters, the wall is indicated by the black box, the dark gray region is for free motion, and the light gray region for motion with collision. The symbols provide examples connecting final and initial parameters: $x_s/d = 0, v_s/v_b = 0 \rightarrow x_f/d = 0, v_f/v_b = 0$ (free motion, circles); $x_s/d = 0, v_s/v_b = 1 \rightarrow x_f/d = 1, v_f/v_b = 1$ (free motion, boxes); $x_s/d = 0, v_s/v_b = 2 \rightarrow x_f/d = 1/2, v_f/v_b = 0$ (collision, triangles).

in our experiment. At this time, the wall has moved a distance d (see Fig. 1), so we get $\alpha = d/\sqrt{t_f}$. Another important quantify is $v_b := d/t_f$, the boundary velocity for no collision until t_f , i.e., a particle with an initial velocity $v_s < v_b$ will not hit the mirror until t_f .

Let us now examine the effect of the mirror with trajectory $x_m(t) = d\sqrt{t/t_f}$ in more detail, allowing for a more general scenario where the initial position of the particle is not necessarily zero but $x(0) = x_s \leq 0$. We are interested in the particle's position x_f and velocity v_f at t_f . It is useful to introduce dimensionless variables to simplify the notation in the following, namely

$$\chi = \frac{x}{d}, \nu = \frac{v}{v_b}, \tau = \frac{t}{t_f}. \quad (3)$$

By a straightforward calculation we get for the position and velocity of the particle at time $\tau = 1$ for $\chi_s \leq 0$:

$$\begin{aligned} \nu_f(\chi_s, \nu_s) &= \begin{cases} \frac{1}{\eta(\chi_s, \nu_s)} - \nu_s & : \nu_s > 1 - \chi_s \\ \nu_s & : \text{otherwise} \end{cases} \\ \chi_f(\chi_s, \nu_s) &= \begin{cases} \chi_s + \frac{1}{\eta(\chi_s, \nu_s)} - \nu_s + 2\nu_s\eta^2(\chi_s, \nu_s) - \eta(\chi_s, \nu_s) & : \nu_s > 1 - \chi_s \\ \chi_s + \nu_s & : \text{otherwise} \end{cases}, \end{aligned}$$

with

$$\eta(\chi_s, \nu_s) = \frac{1}{2\nu_s} \left(1 + \sqrt{1 - 4\chi_s\nu_s} \right). \quad (4)$$

If $\nu_s < 1 - \chi_s$ the particle keeps its initial velocity, i.e., it moves too slowly to collide with the moving-wall before τ_1 , see also Fig. 2. We can also work out the inverse transformation to get the initial position and velocity from the final parameters for $\chi_f < 1$:

$$\begin{aligned} \nu_s(\chi_f, \nu_f) &= \begin{cases} \lambda(\chi_f, \nu_f) - \nu_f & : \chi_f > \nu_f \text{ and } \nu_f \leq 0 \\ \nu_f & : \text{otherwise} \end{cases} \\ \chi_s(\chi_f, \nu_f) &= \begin{cases} \chi_f - \nu_f + \frac{2}{\lambda^2(\chi_f, \nu_f)} \left(\nu_f - \frac{\lambda(\chi_f, \nu_f)}{2} \right) & : \chi_f > \nu_f \text{ and } \nu_f \leq 0 \\ \chi_f - \nu_f & : \text{otherwise} \end{cases}, \end{aligned}$$

with

$$\lambda(\chi_f, \nu_f) = \frac{1}{2(\chi_f - \nu_f)} \left(1 + \sqrt{1 - 4\nu_f(-\nu_f + \chi_f)} \right). \quad (5)$$

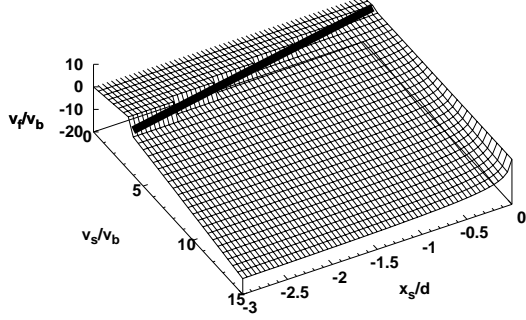


FIG. 3: Final velocity $v_f(x_s, v_s)$, the line at $v_s/v_b = 1 - x_s/d$ separates the regions with or without a collision before t_f .

The function $v_f(x_s, v_s) = v_b \nu_f(x_s/d, v_s/v_b) = v_b \nu_f(\chi_s, \nu_s)$ is important as it provides the extent to which the moving mirror fails to stop the particles when they deviate from the ideal conditions $\chi_s = 0$ and $\nu_s \geq 1$. This function is shown in Fig. 3. Let us examine the case $\nu_s > 1 - \chi_s$ (and $\chi_s \leq 0$), i.e. a collision has occurred before $\tau = 1$: the final velocity is negative, $\nu_f \leq 0$; also

$$\begin{aligned} \frac{\partial \nu_f}{\partial \nu_s} &= -1 - \frac{1}{2\chi_s} \left(\frac{1}{4\chi_s^2} - \frac{\nu_s}{\chi_s} \right)^{-\frac{1}{2}} \\ &= -1 + \frac{1}{\sqrt{1 - 4\nu_s\chi_s}} \\ &< 0, \end{aligned}$$

and

$$\begin{aligned} \frac{\partial \nu_f}{\partial \chi_s} &= \frac{-\frac{1}{2\chi_s^3} + \frac{\nu_s}{\chi_s^2}}{2\sqrt{\frac{1}{4\chi_s^2} - \frac{\nu_s}{\chi_s}}} - \frac{1}{2\chi_s^2} \\ &= \frac{1}{2\chi_s^2} \left(\frac{-\frac{1}{2\chi_s} + \nu_s}{\sqrt{\frac{1}{4\chi_s^2} - \frac{\nu_s}{\chi_s}}} - 1 \right) \\ &\geq 0, \end{aligned}$$

so the absolute value of the final velocity is increasing with increasing $|\chi_s|$ and $|\nu_s|$.

Fig. 3 suggests to us a possible strategy to select the parameters d and t_f and optimize the stopping: assume that the initial parameters x_s and v_s are fixed (they may correspond to estimates of the least favorable values expected or permitted, such as the farthest distance from

the origin allowed by the initial geometry of the launching conditions and a lower bound for the speed). First we choose d and t_f such that

$$v_b = \frac{d}{t_f} \ll v_s.$$

We have for the final velocity

$$v_f(x_s, v_s) = v_b \nu_f \left(\frac{x_s}{d}, \frac{v_s}{v_b} \right) \xrightarrow{d \rightarrow \infty} 0 \quad (v_b \text{ fixed}).$$

According to Fig. 3, this means that if we make d large enough, increasing also t_f so that v_b remains constant, the final velocity goes to zero, even with imperfect conditions. The condition $v_b(1 - x_s/d) < v_s$ should be also satisfied for the chosen d , so that the particle collides with the wall, but this is not a problem because

$$v_b \left(1 - \frac{x_s}{d} \right) \xrightarrow{d \rightarrow \infty} v_b \ll v_s \quad (v_b \text{ fixed}).$$

In the following we shall discuss the more general case in which the initial position and the velocity of the particle are characterized by a probability density $p_s(x_s, v_s)$. The final probability density for position and velocity of the particle is given by

$$p_s(x_f, v_f) = p_s[x_s(x_f, x_f), v_s(v_f, v_f)].$$

In particular we shall consider examples with

$$p_s(x, v) = \frac{1}{N} \exp \left[-\frac{(v - v_0)^2}{2\Delta v^2} - \frac{(x - x_0)^2}{2\Delta x^2} \right]$$

for $x < 0$, and $p_s(x, v) = 0$ for $x \geq 0$ (N being a normalization constant).

The initial probability density p_s for the parameters $x_0/d = -0.04$, $\Delta x/d = 0.008$, $v_0/v_b = 5.0$ and $\Delta v/v_b = 2.0$ is shown in Fig. 4a (solid line). Also the final probability density is shown in Fig. 4a (striped line). The integrated probability densities

$$\begin{aligned} p_{x,s/f}(x) &= \int dv p_{s/f}(x, v) \\ p_{v,s/f}(v) &= \int dx p_{s/f}(x, v) \end{aligned}$$

for this example are shown in Fig. 4b and c. Fig. 4c illustrates the slowing down and narrowing of the final velocity distribution (dashed line) compared to the initial one (solid line). Moreover, a small fraction of particles have not hit the wall: they correspond to the final distribution in the interval $0 < v/v_b < 1$. One more example is

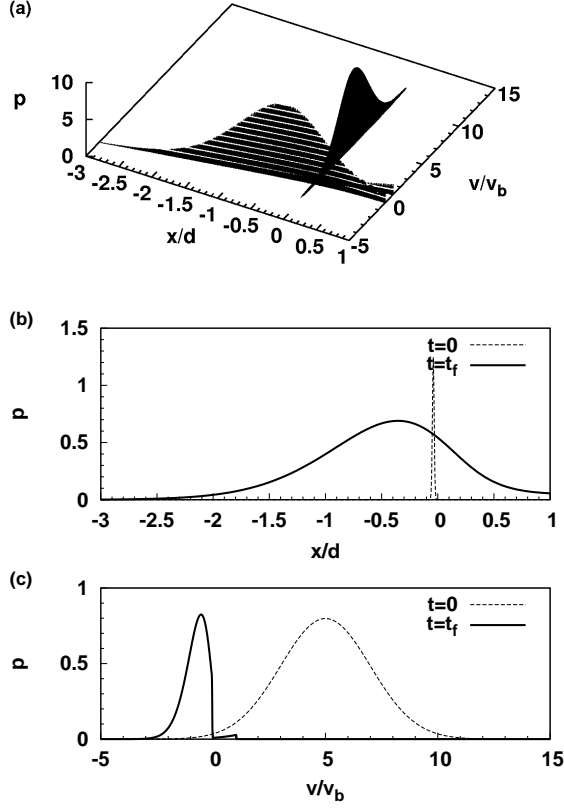


FIG. 4: Classical setting, $x_0/d = -0.04$, $\Delta x/d = 0.008$, $v_0/v_b = 5.0$ and $\Delta v/v_b = 2.0$; (a) initial probability density p_s (solid graph) and final probability density p_f ; (b) $p_{x,s}$ ($t = 0$, scaled by a factor of $1/40$) and $p_{x,f}$ ($t = t_f$); (c) $p_{v,s}$ ($t = 0$, scaled by a factor of 4) and $p_{v,f}$ ($t = t_f$).

shown in Fig. 5, where a rather drastic stopping can be seen. Note that the decrease of the width of the velocity distribution results always in an increase of the width of the position distribution because the phase-space volume is conserved.

III. QUANTUM SETTING

The dimensional Schrödinger equation for the particle and the moving mirror potential is

$$i\hbar \frac{\partial}{\partial t} \psi(x, t) = -\frac{\hbar^2}{2m} \frac{\partial^2}{\partial x^2} \psi(x, t) + V\left(x - d\sqrt{t/t_f}\right) \psi(x, t),$$

where $V(x)$ is the potential of the wall and the mass in the examples below is that of Rubidium ($m_{dim} = 14.19226 \cdot 10^{-26}$ kg). The probability densities do not depend on the mass of the particle classically, but in the quantum case they do. The initial wavefunction is a Gaussian, but not necessarily a minimum-uncertainty-product one,

$$\psi_0(x) = \frac{1}{N} \exp \left\{ -\frac{\mu}{2(1 + 2i\Delta v^2 \mu \delta)} \left[i v_0 (\delta v_0 - 2x) + 2\Delta v^2 \mu ((x - \beta)^2 + 2\delta v_0 \beta) \right] \right\},$$

where $\delta = \sqrt{4\Delta x^2 - 1/(\Delta v^2 \mu^2)}/(2\Delta v)$, and $\beta = x_0 - \delta v_0$, $\mu = m/\hbar$. The form of Heisenberg's uncertainty relation is $\Delta x \Delta v \geq 1/(2\mu)$.

In the calculations we shall use an infinitely high wall, i.e.,

$$V_i(x) = \begin{cases} \infty & : x \geq 0 \\ 0 & : x < 0 \end{cases},$$

as well as a more realistic Gaussian wall, with potential

$$V_G(x) = V_0 \exp[-x^2/(2\Delta x_V^2)].$$

For cold atoms such a potential could be implemented by a detuned laser.

The first example corresponds to the parameters

$$\begin{aligned} x_0 &= -2 \mu\text{m}, \\ \Delta x &= 0.4 \mu\text{m}, \\ v_0 &= 3.125 \text{ cm/s}, \\ \Delta v &= 1.25 \text{ cm/s}. \end{aligned}$$

We choose a boundary velocity $v_b = 0.625 \text{ cm/s} \ll v_0$ and $d = 50 \mu\text{m}$, so that $t_f = 8 \text{ ms}$. We have $x_0/d = 0.04 \ll 1$. The height of the Gaussian potential is set to $V_0/\hbar = 3.75 \cdot 10^6/\text{s}$ and its width is $\Delta x_V = 0.4 \mu\text{m}$, both parameters must be chosen such that the particle is reflected with high probability. The initial and final quantum probability densities are shown in Fig. 6. Qualitatively, we see

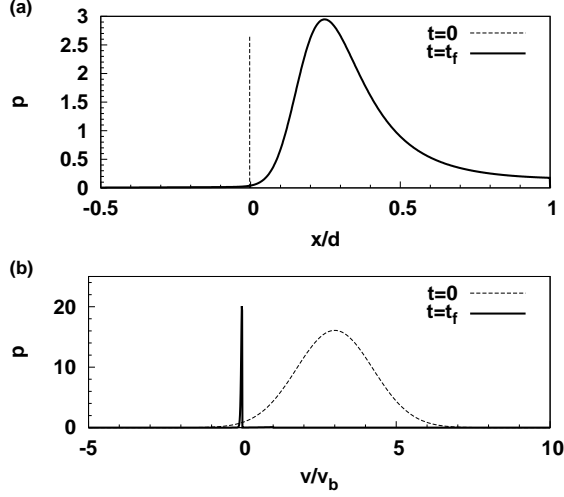


FIG. 5: Classical setting, $x_0/d = -0.003$, $\Delta x/d = 0.0003$, $v_0/v_b = 3.0$ and $\Delta v/v_b = 1.24$; (a) $p_{x,s}$ ($t = 0$, scaled by a factor of $1/500$) and $p_{x,f}$ ($t = t_f$); (b) $p_{v,s}$ ($t = 0$, scaled by a factor of 50) and $p_{x,f}$ ($t = t_f$).

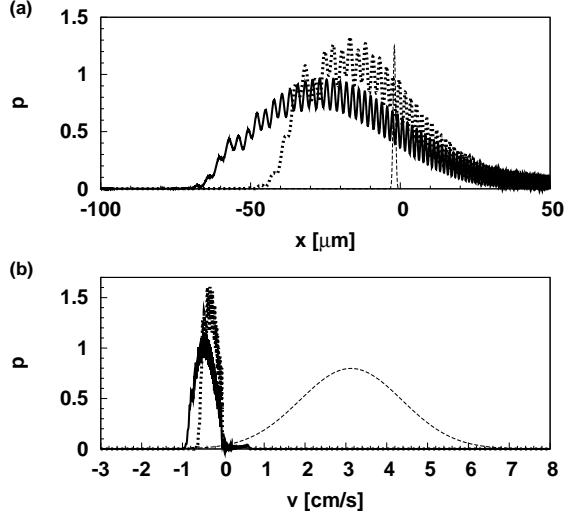


FIG. 6: Quantum setting, see text for parameters; (a) $p_{x,s}$ ($t = 0$, dashed line, scaled by a factor of $1/40$), $p_{x,f}$ with an ideal wall ($t = t_f$, thick solid line), $p_{x,f}$ with a Gaussian wall ($t = t_f$, thick dotted line); (b) $p_{v,s}$ ($t = 0$: scaled by a factor of 4, dashed line), $p_{v,f}$ with an ideal wall ($t = t_f$, thick solid line), $p_{v,f}$ with a Gaussian wall ($t = t_f$, thick dotted line) and $p_{x,f}$ ($t = 1$).

the same result in the quantum case as in the classical case, with quantum interference fringes superimposed.

Another spectacular example can be seen in Fig. 7, which shows the initial and final quantum probability

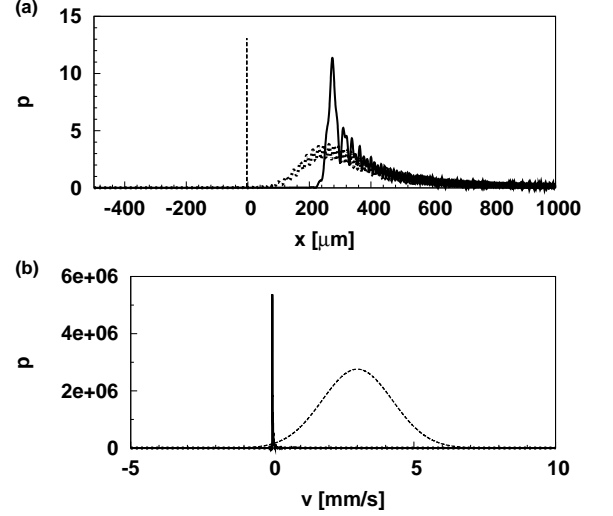


FIG. 7: Quantum setting, see text for parameters; (a) $p_{x,s}$ ($t = 0$, dashed line, scaled by a factor of $1/100$), $p_{x,f}$ with an ideal wall ($t = t_f$, thick solid line), $p_{x,f}$ with a Gaussian wall ($t = t_f$, thick dotted line); (b) $p_{v,s}$ ($t = 0$: scaled by a factor of 100, dashed line), $p_{v,f}$ with an ideal wall ($t = t_f$, thick solid line), $p_{v,f}$ with a Gaussian wall ($t = t_f$, thick dotted line) and $p_{x,f}$ ($t = 1$).

densities for

$$\begin{aligned} x_0 &= -3 \mu\text{m}, \\ \Delta x &= 0.3 \mu\text{m}, \\ v_0 &= 3 \text{ mm/s}, \\ \Delta v &= 1.24 \text{ mm/s}, \\ d &= 1000 \mu\text{m}, \\ t_f &= 1 \text{ s}, \\ v_b &= 1 \text{ mm/s}. \end{aligned}$$

We have $v_b < v_0$ and $x_0/d = 0.003 \ll 1$. The height of the Gaussian potential is set to $V_0/\hbar = 3 \cdot 10^4/\text{s}$ and its width to $\Delta x_V = 0.8 \mu\text{m}$.

IV. SUMMARY

We have proposed a method to stop particles of unknown velocities or ensembles of particles with initial velocity spread by reflecting them from an accelerated wall with trajectory $\sim \sqrt{t}$. For classical particles, the stopping is perfect if they are emitted from the origin at $t = 0$. If the particle starting point is not at the origin or if it is too slow, it is not perfectly stopped in a finite time. Explicit expressions are given for the final velocity; they also show how to mitigate, and even suppress in a limit, the effect of non-ideal initial conditions. We may expect a similar behavior for a quantum wave packet and indeed, using numerical simulations with realistic and experimentally accessible parameters, we have

illustrated the efficiency of the method and discussed its bounds.

Acknowledgments

We acknowledge A. del Campo for discussions and preliminary work. We acknowledge “Acciones Integradas”

of the German Academic Exchange Service (DAAD) & Ministerio de Educación y Ciencia; as well as Grants by Ministerio de Educación y Ciencia (FIS2006-10268-C03-01) and Basque Country University UPV-EHU (GIU07/40). SS and AR acknowledge support by the German Research Foundation (DFG).

-
- [1] A. Steyerl, H. Nagel, F. X. Schreiber, K. A. Steinhauser, R. Gähler, W. Gläser, P. Ageron, J. M. Astruc, W. Drexel, G. Gervais, W. Mampe, Phys. Lett. A **116**, 347 (1986).
 - [2] A. Steane, P. Szriftgiser, P. Desbiolles, J. Dalibard, Phys. Rev. Lett. **74**, 4972 (1995)
 - [3] M. Arndt, P. Szriftgiser, J. Dalibard, A.M. Steane, Phys. Rev. A **53**, 3369 (1996).
 - [4] A. Libson *et al.*, New. J. Phys. **8**, 77 (2006).
 - [5] G. Reinaudi *et al.*, Eur. Phys. J. D. **40**, 405 (2006).
 - [6] A. del Campo, J. G. Muga, and M. Kleber, Phys. Rev. A **77**, 013608 (2008)
 - [7] E. Narevicius, A. Libson, M. F. Riedel, C. G. Parthey, I. Chavez, U. Even and M. G. Raizen, Phys. Rev. Lett. **98**, 103201 (2007).